Journal of Solid State Chemistry **163,** 27–32 (2002)
doi:10.1006/jssc.2001.9348, available online at http://www.idealibrary.com on IDEAL®

Preparation of Lead–Calcium Hydroxyapatite Solid Solutions by a Wet Method Using Acetamide

Akemi Yasukawa,[1] Kaori Kamiuchi, Takashi Yokoyama, and Tatsuo Ishikawa

School of Chemistry, Osaka University of Education, Asahigaoka 4-698-1, Kashiwara-shi, Osaka 582-8582, Japan

Received April 4, 2001; in revised form August 3, 2001; accepted August 9, 2001

Lead–calcium hydroxyapatite solid solutions with different Pb/(Pb + Ca) molar ratios (X_{Pb}) were prepared by a wet method using acetamide (AA). The crystal phase and structure of the products depended on the aging period (t_a), Pb/(Pb + Ca) molar ratio ([X_{Pb}]), and AA concentration ([AA]) of the starting solution. At [AA] = 1.6 mol dm^{-3} and t_a = 6 days, the large needle-like PbCaHap particles were formed from solutions at [X_{Pb}] = 0–0.6 and 0.9–1. Under the other AA concentrations and aging periods, pure PbCaHap particles could be obtained in a narrower region of [X_{Pb}]; e.g., PbCaHap was formed from solutions at [AA] = 0.8 mol dm^{-3}, t_a = 6 days, and [X_{Pb}] = 0–0.1, 0.4–0.5, and 0.9–1.

INTRODUCTION

Calcium hydroxyapatite (designated as CaHap), $Ca_{10}(PO_4)_6(OH)_2$, is a primary constituent of biological hard tissues in animal organisms. Ca^{2+} ion sites can be replaced by various divalent cations including Sr^{2+}, Ba^{2+}, Pb^{2+}, Cd^{2+}, etc. (1–4). When these harmful heavy metal ions are taken into an organism, there is a possibility that they accumulate in the body by forming hydroxyapatite (designated as Hap) solid solutions with vital CaHap. Ion exchangeability of CaHap may be employed for removal of noxious metal ions from waste fluid. Thus, the exchange of Ca^{2+} ions in CaHap with harmful ions such as Pb^{2+} is an interesting subject in medical and environmental sciences. To investigate the selectivity of cation exchange in a Hap crystal, we have prepared various Hap solid solutions, such as strontium–calcium hydroxyapatite (SrCaHap) (5), magnesium–calcium hydroxyapatite (MgCaHap) (6), and barium–strontium hydroxyapatite (BaSrHap) (7). According to a series of these studies, the preferences of cation sites are in the order of $Mg^{2+} < Ca^{2+}$ and $Ba^{2+} < Sr^{2+} < Ca^{2+}$. To obtain further information on the ion selectivity of Hap, preparation and characterization of lead–calcium hydroxyapatite (PbCaHap) solid solution is significant.

Many investigators synthesized PbCaHap particles by the co-precipitation method (8–13), solid state reaction (14), and ion-exchange method (15,16). The sizes of the PbCaHaps reported in their papers are 12×60 nm (10) and 50×250 nm (11), and there are neither particle sizes nor TEM pictures in other papers (8,9,12–16).

We previously prepared needle-like CaHap and PbHap particles by a wet method using acetamide (CH_3CONH_2, designated as AA) (17,18). AA is hydrolyzed slowly at an elevated temperature by the following reaction,

$$CH_3CONH_2 + H_2O \rightarrow CH_3COOH + NH_3, \qquad [1]$$

and the resultant NH_3 raises the solution pH to yield Hap particles. Slow hydrolysis of AA forms larger (micro meter size) and more crystallized Hap particles than ones prepared without AA (5, 6). In the present study, we prepared various PbCaHap solid solutions ($Pb_XCa_{10-X}(PO_4)_6(OH)_2$, $X = 0$–1) by changing the synthetic conditions such as aging period, Pb/(Pb + Ca) molar ratio, and AA concentration in the starting solution. We searched the conditions for the formation of PbCaHap and characterized the products in detail.

EXPERIMENTAL

Materials

PbCaHap solid solutions with various Pb/(Pb + Ca) molar ratios (designated as X_{Pb}) of 0–1 were synthesized by a wet method using AA as follows. Table 1 lists the preparation conditions of the materials by aging the solution at an AA concentration (designated as [AA]) of 1.6 mol dm^{-3} for 6 days. A total of 100 cm^3 of solutions with different Pb/(Pb + Ca) molar ratios in starting solution (designated as [X_{Pb}]) of 0–1 was prepared by dissolving various amounts of $Pb(NO_3)_2$ and $Ca(NO_3)_2 \cdot 4H_2O$ in water. To the solutions were added 50 cm^3 of the buffer solution containing NH_4NO_3, AA solid, and 25 cm^3 of

[1] To whom correspondence should be addressed. Fax: + 81-729-78-3394. E-mail: yasukawa@cc.osaka-kyoiku.ac.jp.

0022-4596/02 $35.00

TABLE 1
Synthetic Conditions and Crystal Phases of the Products

$[X_{Pb}]$ in solution	$[HNO_3]$ (mol dm^{-3})	pH before aging	pH after aging	X_{Pb} in particles	(Pb + Ca)/P	Crystal phase by XRD
0	0.038	2.93	5.02	0	1.53	CaHAP
0.1	0.162	1.25	4.76	0.12	1.52	PbCaHAP
0.2	0.191	1.18	4.73	0.24	1.51	PbCaHAP
0.3	0.220	1.03	4.72	0.37	1.54	PbCaHAP
0.4	0.232	1.07	4.69	0.50	1.56	PbCaHAP
0.5	0.258	0.99	4.70	0.64	1.59	PbCaHAP
0.6	0.273	0.93	4.67	0.76	1.56	PbCaHAP
0.7	0.292	0.91	4.67	0.78	—	PbCaHAP + β-$(Pb,Ca)_9(PO_4)_6$ + unknown
0.8	0.302	0.91	4.64	0.87	—	PbCaHAP + β-$(Pb,Ca)_9(PO_4)_6$ + unknown
0.9	0.318	0.88	4.65	0.98	1.66	PbCaHAP
1	0.320	0.88	4.63	1	1.63	PbHAP

Note. $[Pb(NO_3)_2 + Ca(NO_3)_2 \cdot 4H_2O]$: 5.0×10^{-2} mol dm^{-3}; $[(NH_4)_2HPO_4]$: 3.0×10^{-2} mol dm^{-3}; $[NH_4NO_3]$: 0.10 mol dm^{-3}; [AA]: 1.6 mol dm^{-3}. The aging temperature and period were 100°C and 6 days.

$(NH_4)_2HPO_4$ solution. White precipitates were formed. HNO_3 solution (2 mol dm^{-3}) was added untill the resulting precipitates were redissolved. Finally, the solution volume was adjusted to 250 cm^3 by adding water. The component of each solution is shown in Table 1. The solutions thus prepared were aged in 500 cm^3 screw-capped polypropylene vessels at 100°C for 6 days. The supernatant pH at room temperature was measured before and after the aging. The precipitates formed were filtered off, washed with 1 dm^3 of water, and finally dried in an air oven at 70°C for 16 h.

To know the influences of [AA] and the aging period (t_a), we prepared particles from the solutions at $[X_{Pb}] = 0$–1 by changing [AA] from 0.4 to 2.0 mol dm^{-3} and t_a from 3 to 12 days in addition to the synthetic condition mentioned above.

The water used for preparation of samples was deionized–distilled and further purified by boiling under an N_2 atmosphere to remove CO_2.

Characterization

The materials synthesized were characterized as follows. Their crystal phases were identified by powder X-ray diffraction (XRD) using a diffractometer (Rigaku Geigerflex 2013) with Ni-filtered Cu$K\alpha$ radiation (30 kV and 15 mA). A scanning electron microscope (SEM, JEOL JSM-840A) was used to ascertain the morphology of the products. Transmission infrared (IR) spectra were taken by a KBr method using a Fourier transform infrared spectrometer (FTIR, Nicolet, Protégé 460). The sample disks for IR were prepared by adding 0.4 mg of sample to 100 mg of KBr. Pb^{2+}, Ca^{2+}, and PO_4^{3-} contents were assayed using an inductively coupled plasma spectrometer (ICP, Seiko SPS 1200 AR) by first dissolving in HNO_3. The specific surface areas were evaluated by fitting the BET equation to the N_2 adsorption isotherms recorded by a computer-aided automatic volumetric apparatus at the boiling point of nitrogen. Before the adsorption, the samples were treated at 300°C under 10^{-3} Torr for 2 h.

RESULTS AND DISCUSSION

Pb, Ca, and P Contents

$[X_{Pb}]$ of the starting solutions and X_{Pb} of the obtained particles are shown in Table 1 for the samples prepared from the solutions at [AA] = 1.6 mol dm^{-3} and $t_a = 6$ days. X_{Pb} of all the materials formed at $[X_{Pb}] = 0.1$–0.9 is more than $[X_{Pb}]$. This indicates that Pb^{2+} ions more easily enter cation sites of the crystal compared to Ca^{2+} ions. We have found that the preference of cation sites of the SrCaHap crystal is $Sr^{2+} < Ca^{2+}$ (5). It is generally said that the cationic selectivity of Hap depends on the radii of the cations (3). The radii of Ca^{2+} and Sr^{2+} ions are 0.100 and 0.118 nm (19), respectively. The ion radius of Pb^{2+} is 0.119 nm (19), close to that of Sr^{2+} ions. Therefore, the selectivity of cation sites depends on not only ionic radii but also other factors: charge, polarizability, and ability to form partial covalent bonds. The preference of Pb^{2+} ions in PbCaHap has been explained by the last factor (12). Since lead nitrate precipitates at a lower pH than calcium nitrate, only Pb^{2+} ions should precipitate at the initial stage of the particle forming. This may also be related to the X_{Pb} in the particles.

The (Pb + Ca)/P molar ratio of the particles is also shown in Table 1. All the ratios are less than the stoichiometric ratio of 1.67, meaning the formation of cation-deficient PbCaHap.

Crystal Structure

The crystal phases of the samples prepared from the solutions at [AA] = 1.6 mol dm^{-3}, different $[X_{Pb}]$, and

$t_a = 6$ days were examined by XRD. The obtained patterns and the crystal phases are shown in Fig. 1 and Table 1, respectively. The crystal phases and peak intensities of the materials depend on X_{Pb}. The highly crystallized products with $X_{Pb} = 0$ and 1 are identified as CaHap (JCPDS 9-432) and PbHap (JCPDS 24-686), respectively (Fig. 1 (a) and 1(f)). By doping a small amount of Pb^{2+} ions into CaHap, the crystallinity of the particles is markedly reduced as shown in pattern (b) of the sample with $X_{Pb} = 0.12$. As X_{Pb} increases, the peaks of CaHap shift to that of PbHap and all the patterns show only one set of Hap peaks except for the samples with $X_{Pb} = 0.78$ and 0.87. Therefore, the materials with $X_{Pb} = 0.12$–0.76 and 0.98 are identified to PbCaHap solid solution (JCPDS 40-1495, 40-1496, and 40-1497). The products with $X_{Pb} = 0.78$ and 0.87 are a mixture of PbCaHap (○), β-$(PbCa)_9(PO_4)_6$ (JCPDS 33-768) (□), and unknown material (▽) as seen from XRD peaks in Fig. 1 (e), although the pattern of the latter product is not shown here. The peaks of the unknown material almost agree with those of $PbH_2P_2O_7$ (JCPDS 12-5). However, since this material is known to hardly form under such moderate synthetic conditions as at atmospheric pressure and 100°C employed in the present study, this material is not identified for the moment.

PbCaHap with $X_{Pb} = 0.64$ (Fig. 1(d)) shows the best crystallinity out of all the PbCaHap solid solutions except for CaHap (pattern (a)) and PbHap (pattern (f)). Hap crystal has two cation sites, (I) and (II), in a ratio of 4:6 (2, 3). These sites are established in being occupied respectively by smaller and larger cations in Hap solid solution containing two kinds of cations (3). It has been reported that Pb^{2+} and Ca^{2+} ions of PbCaHap prepared by the co-precipitation method are located respectively in (II) and (I) sites (3, 8, 12). Consequently, PbCaHap with $X_{Pb} \approx 0.6$ of which Pb^{2+} and Ca^{2+} ions are mainly in (II) and (I) sites, respectively, is most stable for exhibiting the highest crystallinity.

Unit cell dimensions a (○) and c (□) of the products calculated from XRD peaks are shown in Fig. 2. With the increase of X_{Pb}, dimensions a and c increase from 0.94 to 0.99 nm and from 0.69 to 0.75 nm, respectively, owing to the exchange of Ca^{2+} ion (0.100 nm) with larger Pb^{2+} ion (0.119 nm) in Hap crystal. The variation of dimension a has a break at $X_{Pb} = 0.8$. Such a break reported by Engel *et al.* was explained by localization of Pb^{2+} and Ca^{2+} ions in (II) and (I) sites, respectively (12). In the present study, mixing of β-$(PbCa)_9(PO_4)_6$ and unknown material to PbCaHap may also relate to the break of variation of dimension a.

The crystallite sizes (L_{300}) of the particle, evaluated from the half height width of XRD peaks due to the (300) plane shown in Fig. 1 using the Scherrer equation (20), are plotted against X_{Pb} by circle symbols in Fig. 3. The L_{300} value is remarkably reduced from ca. 80 nm at $X_{Pb} = 0$ (CaHap) to 17 nm at $X_{Pb} = 0.12$. As X_{Pb} increases from 0.12 to 1, L_{300} markedly grows to 254 nm at $X_{Pb} = 1$ (PbHap). This result is conceivably ascribed to the following facts: Hap solid solution containing two kinds of cations is less crystalline than Hap containing one kind of cations and the crystallinity of PbCaHap is enhanced with the increase of X_{Pb}.

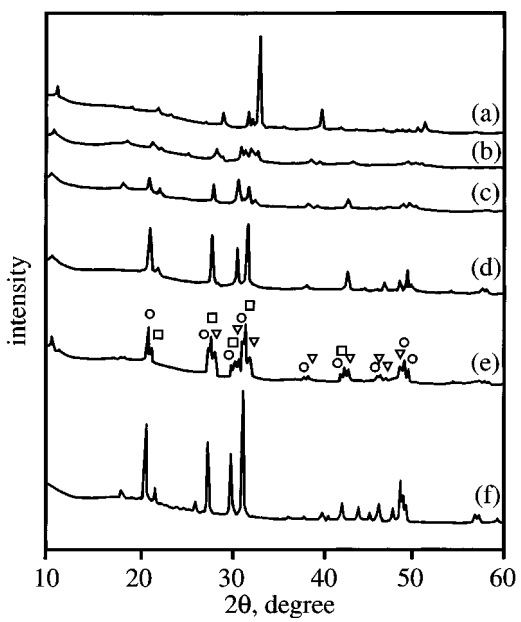

FIG. 1. XRD patterns of the materials with different X_{Pb} formed from solutions at [AA] = 1.6 mol dm^{-3} and $t_a = 6$ days: (a) $X_{Pb} = 0$, (b) 0.12, (c) 0.37, (d) 0.64, (e) 0.78, and (f) 1. (○) PbCaHap, (□) β-$(PbCa)_9(PO_4)_6$ and (▽) unknown material.

Morphology

Figure 4 displays SEM images of the products with various X_{Pb} values. Well-crystalline needle-like particles are seen in each picture. The samples with $X_{Pb} = 0.12$ are the finest and thinnest (picture (b)). The particles grow with

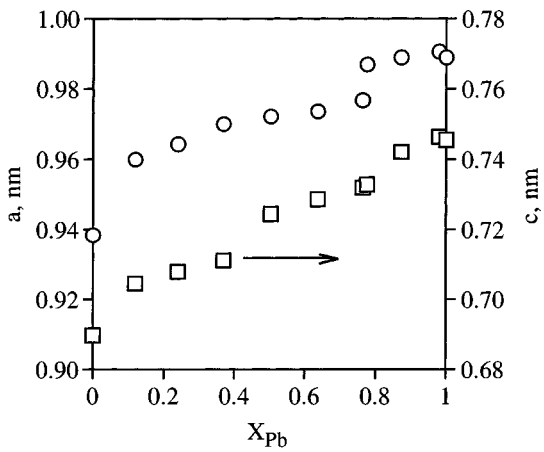

FIG. 2. Unit-cell dimensions vs X_{Pb}: (○) a and (□) c.

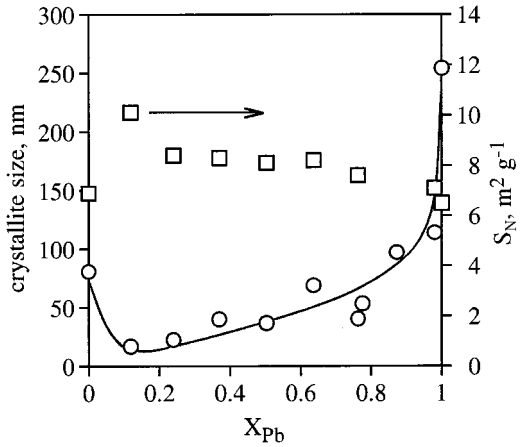

FIG. 3. Crystallite size (L_{300}) calculated from XRD peak due to (300) plane, and specific surface area (S_N) of PbCaHAP particles vs X_{Pb}: (○) L_{300} and (□) S_N.

increasing X_{Pb} from 0.12 to 1 and the largest ones with $X_{Pb} = 1$ are more than 13×550 μm (picture (e)). In picture (d) of the products with $X_{Pb} = 0.87$, irregularly shaped particles (shown by an arrow) coexist with needle-like ones; the former particles are mixtures of β-$(PbCa)_9(PO_4)_6$ and unknown phosphates and the latter ones are PbCaHap as identified by XRD.

N_2 Adsorption

The specific surface area (S_N) of PbCaHap solid solutions estimated from the adsorption isotherms of N_2 is plotted against X_{Pb} by square symbols in Fig. 3. S_N values of all the products are small, 7–10 $m^2 g^{-1}$. This result agrees well with the large particles seen in SEM pictures in Fig. 4.

According to the t-plot analysis (21) of N_2 adsorption isotherms, PbCaHap solid solutions are not microporous. The pore size distribution curves of the materials, calculated by applying the Dollimore–Heal method (22) to the N_2 adsorption isotherms, revealed that mesopores with diameters of 3–5 nm develop in the particles and can be regarded as the cavities among the particles.

IR Spectra

To obtain information on the anionic species of the products, their IR spectra were taken by a KBr method (Fig. 5). Spectrum (a) of the particles with $X_{Pb} = 0$ is characteristic of CaHap, showing the P–O stretching vibrations of PO_4^{3-} ions at 1089, 1031, and 963 cm^{-1} and their deformation vibrations at 604 and 563 cm^{-1} (23–25). The band at 866 cm^{-1} is assigned to HPO_4^{2-} ions contained in cation-deficient CaHap, $Ca_{10-X}(HPO_4)_X(PO_4)_{6-X}(OH)_{2-X}$ (3). The band at 635 cm^{-1} is assigned to the librational motion of OH^- ions (24, 25). With the increase of X_{Pb}, the bands at

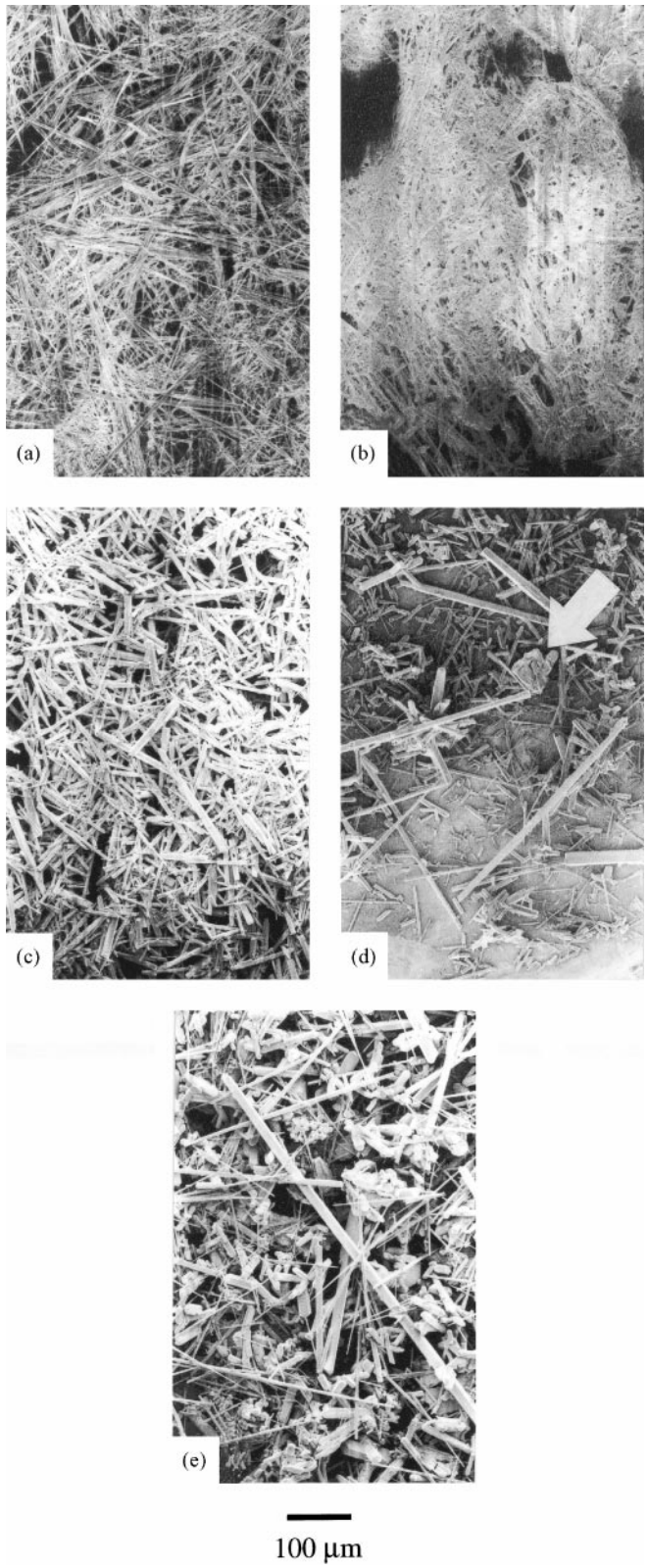

FIG. 4. SEM pictures of the materials with different X_{Pb} formed from solutions at [AA] = 1.6 mol dm^{-3} and $t_a = 6$ days; $X_{Pb} =$ (a) 0, (b) 0.12, (c) 0.76, (d) 0.87, and (e) 1.

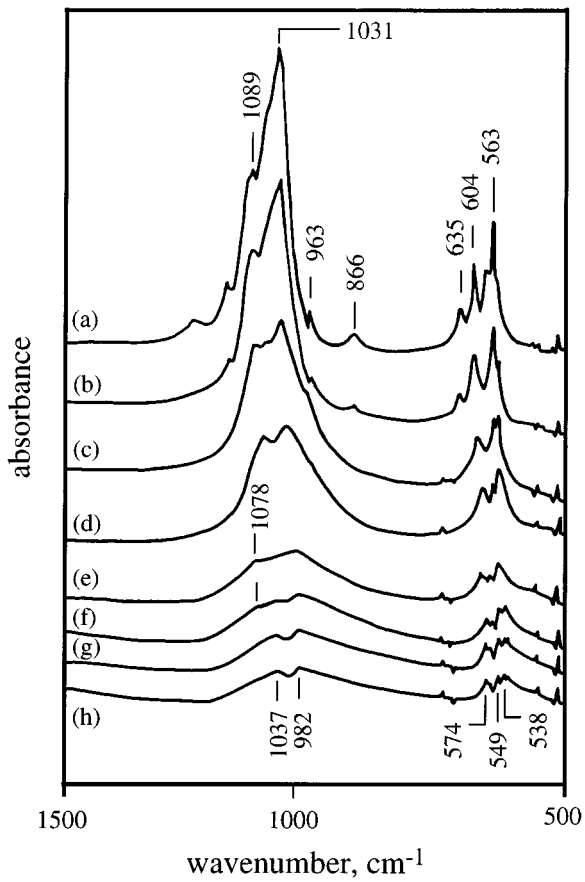

FIG. 5. IR spectra of the materials with different X_{Pb} formed from solutions at [AA] = 1.6 mol dm^{-3}, and t_a = 6 days; X_{Pb} = (a) 0, (b) 0.12, (c) 0.37, (d) 0.64, (e) 0.78, (f) 0.87, (g) 0.98, and (h) 1.

1089, 1031, and 604 cm^{-1} shift respectively to 1037, 982, and 574 cm^{-1}, the bands at 963, 866, and 635 cm^{-1} disappear, and the 563-cm^{-1} band splits into two bands at 549 and 538 cm^{-1}. Spectrum (h) is characteristic of PbHap (26, 27). All the bands are diminished with the increase of X_{Pb} due to the scattering of IR beam by the large particles observed in the SEM pictures in Fig. 4. There is a weak shoulder at 1078 cm^{-1} in the spectra of the materials, which are not pure PbCaHap but a mixture of PbCaHap and the other phosphates (spectra (e) and (f)), which is assigned to the stretching vibrations of PO_4^{3-} of the phosphates other than PbCaHap (27).

Crystal Phase

The influence of [AA] on the products was investigated by preparing the particles at different [X_{Pb}] and [AA] = 0.4–2.0 mol dm^{-3}. The crystal phases of the products determined by XRD are shown in Fig. 6(A). As shown in this figure, PbCaHap solid solution (○) is formed at [AA] = 1.6 mol dm^{-3} and [X_{Pb}] = 0–0.6 and 0.9–1. The [X_{Pb}] region of PbCaHap formation with [AA] = 0.4–1.2 and 2.0 mol dm^{-3} is narrower than that with [AA] = 1.6 mol dm^{-3}.

It is noteworthy that PbCaHap solid solutions can be prepared at [X_{Pb}] = 0.4 and 0.5 under all the concentrations at [AA] = 0.4–2.0 mol dm^{-3}. At [AA] = 1.6 mol dm^{-3}, X_{Pb} of the particles formed at [X_{Pb}] = 0.4 and 0.5 are 0.52 and 0.64, respectively; X_{Pb} is larger than [X_{Pb}]. As already mentioned, Hap crystal has cationic (I) and (II) sites at a ratio of 4:6 (2, 3). In PbCaHap, Ca^{2+} and Pb^{2+} ions should exist in (I) and (II) sites, respectively (3, 8, 12). Therefore, PbCaHap solid solution is most stable and formed easily at $X_{Pb} \approx 0.6$, where Pb^{2+} and Ca^{2+} ions are mainly localized to (II) and (I) sites, respectively.

To know the influence of t_a on the products, the particles were prepared by varying t_a from 3 to 12 days at [AA] = 1.6 mol dm^{-3}. The crystal phases of the products determined by XRD are shown in Fig. 6(B). At [X_{Pb}] ≤ 0.5 PbCaHap (○) can be obtained under all the conditions at t_a = 3–12 days.

As is seen in Figs. 6(A) and 6(B), no PbCaHap could be synthesized at [X_{Pb}] = 0.7–0.8 independent of [AA] and

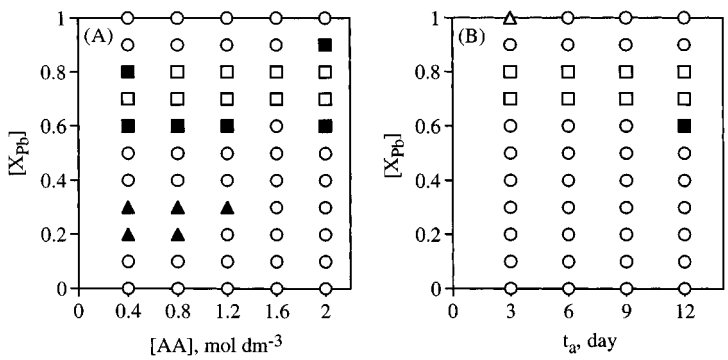

FIG. 6. The crystal phases of the materials obtained at different synthetic conditions. (A) At different [X_{Pb}], different [AA], and t_a = 6 days (B) At different [X_{Pb}], [AA] = 1.6 mol dm^{-3}, and different t_a: (○) PbCaHAP, (▲) PbCaHap–(PbCa)HPO$_4$ mixture, (■) PbCaHap–β-(PbCa)$_9$(PO$_4$)$_6$ mixture, (△) PbCaHap–α-(PbCa)$_9$(PO$_4$)$_6$ mixture, and (□) PbCaHap–β-(PbCa)$_9$(PO$_4$)$_6$–unknown mixture.

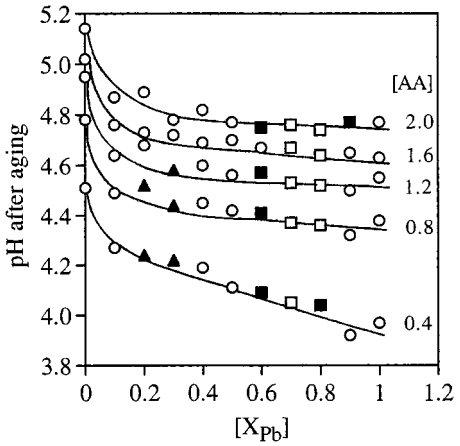

FIG. 7. The relationship between pH after aging for 6 days, and $[X_{Pb}]$ at different [AA]: (○) PbCaHAP, (▲): PbCaHap–$(PbCa)HPO_4$ mixture, (■) PbCaHap–β-$(PbCa)_9(PO_4)_6$ mixture, and (□) PbCaHap–β-$(PbCa)_9(PO_4)_6$–unknown mixture.

t_a in the present study. The crystal phases obtained depend more strongly on $[X_{Pb}]$ than [AA] and t_a.

pH after Aging

Figure 7 shows the solution pH after aging at $t_a = 6$ days and different [AA] as a function of $[X_{Pb}]$. On increasing [AA], more NH_3 is produced in the hydrolysis of AA, leading to a rise of solution pH. CaHap and PbHap are known to form in alkaline or neutral conditions, such as pH 8.5–9.5 (28), 8.5–11.0 (29), and 6.0–9.0 (3) for CaHap and 6.8 (30) and 12 (11) for PbHap. PbCaHap has been obtained at pH 6.5 (9), 11 (10), and 12 (8, 11). Therefore, it is novel that PbCaHap was produced at such a low pH of 3.92–5.22 in the present study. As is seen from this figure, the crystal phases of the products are determined not by pH but by $[X_{Pb}]$ and [AA] of the synthetic solution.

CONCLUSIONS

The large needle-like PbCaHap solid solutions with various X_{Pb} of 0–0.76 and 0.98–1 were prepared by the wet method using AA. When the synthetic conditions such as $[X_{Pb}]$, [AA], and t_a were changed, the crystal phases of the materials varied: PbCaHap, the mixtures of PbCaHap–$(PbCa)HPO_4$, PbCaHap–β-$(PbCa)_9(PO_4)_6$, and PbCaHap–β-$(PbCa)_9(PO_4)_6$–unknown material. PbCaHap particles could not be prepared at $[X_{Pb}] = 0.7$–0.8 independently of the other synthetic conditions.

ACKNOWLEDGMENTS

The authors are grateful to Associate Professor Kazuhiko Kandori in Osaka University of Education for his valuable suggestions and comments. This study was supported in part by the Nippon Sheet Glass Foundation and by the Grant-in-Aid for Science Research Fund (C) from the Ministry of Education, Science, Sports and Culture, Japanese Government.

REFERENCES

1. R. Z. LeGeros, "Calcium Phosphates in Oral Biology and Medicine." Karger, Basle, 1991.
2. P. W. Brown and B. Constantz, "Hydroxyapatite and Related Materials." CRC Press, Boca Raton, FL, 1994.
3. J. C. Elliott, "Structure and Chemistry of the Apatites and Other Calcium Orthophosphates." Elsevier, Amsterdam, 1994.
4. R. W. Mooney and M. A. Aia, *Chem. Rev.* **61,** 433 (1961).
5. T. Ishikawa, H. Saito, A. Yasukawa, and K. Kandori, *J. Chem. Soc. Faraday Trans.* **89,** 3821 (1993).
6. A. Yasukawa, S. Ouchi, K. Kandori, and T. Ishikawa, *J. Mater. Chem.* **6,** 1401 (1996).
7. A. Yasukawa, M. Kidokoro, K. Kandori, and T. Ishikawa, *J. Colloid Interface Sci.* **191,** 407 (1997).
8. R. M. H. Verbeeck, C. J. Lassuyt, H. J. M. Heijligers, F. C. M. Driessens, and J. W. G. A. Vrolijk, *Calcif. Tissue Int.* **33,** 243 (1981).
9. M. Müller, *Helv. Chim. Acta* **30,** 2069 (1947).
10. S. V. C. Rao and N. S. Chickerur, *J. Inst. Chem. (India)* **44,** 177 (1972).
11. T. S. B. Narasaraju, R. P. Singh, and V. L. N. Rao, *J. Inorg. Nucl. Chem.* **34,** 2072 (1972).
12. G. Engel, F. Krieg, and G. Reif, *J. Solid State Chem.* **15,** 117 (1975).
13. Y. Matsumura, S. Sugiyama, H. Hayashi, and J. B. Moffat, *J. Solid State Chem.* **114,** 138 (1995).
14. A. Bigi, A. Ripamonti, S. Brückner, M. Gazzano, N. Roveri, and S. A. Thomas, *Acta Crystallogr. B* **45,** 247 (1989).
15. M. Miyake, K. Ishigaki, and T. Suzuki, *J. Solid State Chem.* **61,** 230 (1986).
16. Y. Matsumura, J. B. Moffat, S. Sugiyama, H. Hayashi, N. Shigemoto, and K. Saitoh, *J. Chem. Soc. Faraday Trans.* **90**(14), 2133 (1994).
17. A. Yasukawa, H. Takase, K. Kandori, and T. Ishikawa, *Polyhedron* **13,** 3071 (1994).
18. A. Yasukawa, T. Kunimoto, K. Kamiuchi, K. Kandori, and T. Ishikawa, *J. Mater. Chem.* **9,** 1825 (1999).
19. R. D. Shannon, *Acta Crystallogr. A* **32,** 751 (1976).
20. P. Gallezot, "Catalysis, Science and Technology," Vol. 5. Springer-Verlag, Berlin, 1983.
21. B. C. Lippens and J. H. de Boer, *J. Catal.* **4,** 319 (1965).
22. D. Dollimore and G. R. Heal, *J. Appl. Chem.* **14,** 109 (1964).
23. W. E. Klee and G. Engel, *J. Inorg. Nucl. Chem.* **32,** 1837 (1970).
24. C. B. Baddiel and E. E. Berry, *Spectrochim. Acta.* **22,** 1407 (1966).
25. B. O. Fowler, *Inorg. Chem.* **13,** 194 (1974).
26. G. Engel and W. E. Klee, *J. Solid State Chem.* **5,** 28 (1972).
27. V. M. Bhatnagar, *Rav. Roumaine Chim.* **16,** 1513 (1971).
28. E. C. Moreno, T. M. Gregory, and W. E. Brown, *J. Res. Natl. Bur. Stand. A* **72,** 773 (1968).
29. H. Monma, *Shokubai*, **27,** 237 (1985).
30. R. Klement, *Z. Anorg. Allg. Chem.* **237,** 161 (1938).